Online Parameterization of Lumped Thermal Dynamics in Cylindrical Lithium Ion Batteries for Core Temperature Estimation and Health Monitoring

Xinfan Lin, Hector E. Perez, Jason B. Siegel, Anna G. Stefanopoulou, *Fellow, IEEE*, Yonghua Li, R. Dyche Anderson, Yi Ding and Matthew P. Castanier

***Abstract*—Lithium ion batteries should always be prevented from overheating and hence thermal monitoring is indispensable. Since only the surface temperature of the battery can be measured, a thermal model is needed to estimate the core temperature of the battery, which can be higher and more critical. In this paper, an online parameter identification scheme is designed for a cylindrical lithium ion battery. An adaptive observer of the core temperature is then designed based on the online parameterization methodology and the surface temperature measurement. A battery thermal model with constant internal resistance is explored first. The identification algorithm and the adaptive observer is validated with experiments on a** $2.3Ah$ **26650 lithium iron phosphate/graphite battery. The methodology is later extended to address temperature dependent internal resistance with non-uniform forgetting factors. The capability of the methodology to track the long term variation of the internal resistance is beneficial for battery health monitoring.**

***Index Terms*—Lithium ion battery, core temperature, adaptive estimation, state of health.**

I. Introduction

LITHIUM ion batteries have been widely considered as an energy storage device for hybrid electric vehicles (HEV), plug-in hybrid electric vehicles (PHEV) and battery electric vehicles (BEV). Thermal management in vehicular applications is a critical issue for lithium ion batteries because of their narrow operating temperature range. An accurate prediction of the battery temperature is the key to maintaining safety, performance, and longevity of these Li-ion batteries.

Existing high fidelity thermal models can predict the detailed temperature distribution throughout the cell [1], [2], [3], [4]. However, these models are not suitable for onboard application due to their high computational intensity. Reduced order models typically use one single temperature, the bulk (or average) temperature, to capture the lumped thermal dynamics of the cell [4], [5], [6], [7]. Even though the single temperature approximation is computationally efficient, it might lead to over-simplification since the temperature in the battery core can be much higher than in the surface [8].

Lumped thermal models capturing both the surface and the core temperatures of the cell have also been studied in [8] and [9]. Such simplified models are efficient for onboard application due to their limited number of states. The accuracy of the model parameters is of great importance since it determines the accuracy of the core temperature estimation. Model parameters can be approximated based on the geometry of the battery and the volume averaging physical properties of its components [9], but such approximation may not be accurate due to the complicated layered structure of the cell and the interfaces between the layers. The parameters can also be determined by fitting the model to the data obtained from experiments [8], involving designed input excitation and measurement of the battery core temperature. This laboratory-oriented parameterization is invaluable for determining the initial values of parameters. However, some of the parameters, such as the internal resistance, may change over the battery lifetime due to degradation. In this case, parameter mismatch leads to inaccurate temperature estimation, and thus identification of present value of the parameters is needed.

A recursive parameter identification scheme is designed in this paper to automatically identify the thermal model parameters based on the signals commonly measured in a vehicle battery management system. The algorithm is simple enough to run on a typical automotive onboard controller. An adaptive observer is then designed for the core temperature estimation. A lumped battery model with constant internal resistance is investigated first, where the least square algorithm is sufficient for identification. In reality, the internal resistance of the battery can be temperature and/or state of charge (SOC) dependent [5], [10], [11] and hence time-varying. The pure least square algorithm may cause errors to the identification if the actual parameters are non-constant. Non-uniform forgetting factors are augmented to the least square algorithm to address the issue of time-varying internal resistance.

Apart from the short-term variability due to conditions such as temperature, the internal resistance of the lithium ion battery may also increase over lifetime due to degradation. This is because the solid electrolyte interphase (SEI) may grow in thickness [12], [13], [14] and reduce the conductivity of

X. Lin, H. Perez, J. Siegel and A. Stefanopoulou are with the Department of Mechanical Engineering, University of Michigan, Ann Arbor, MI 48109, USA e-mail: (xflin@umich.edu, heperez@umich.edu, siegeljb@umich.edu and annastef@umich.edu).

Y. Li and R. D. Anderson are with the Vehicle and Battery Controls Department, Research and Advanced Engineering, Ford Motor Company, Dearborn, MI 48121, USA e-mail: (yli19@ford.com and rander34@ford.com).

Y. Ding and M. Castanier are with the U.S. Army Tank Automotive Research, Development, and Engineering Center (TARDEC), Warren, MI 48397, USA e-mail: (matthew.p.castanier.civ@mail.mil and yi.ding8.civ@mail.mil).

Manuscript received March 6, 2012; revised July 31, 2012.

Report Documentation Page

Form Approved
OMB No. 0704-0188

1. REPORT DATE	2. REPORT TYPE	3. DATES COVERED
13 MAR 2012	**Journal Article**	**10-10-2011 to 08-02-2012**

4. TITLE AND SUBTITLE	5a. CONTRACT NUMBER
Online Parameterization of Lumped Thermal Dynamics in Cylindrical Lithium Ion Batteries for Core Temperature Estimation and Health Monitoring	**W56H2V-04-2-0001**
	5b. GRANT NUMBER
	5c. PROGRAM ELEMENT NUMBER
6. AUTHOR(S)	5d. PROJECT NUMBER
Xinfan Lin; Hector Perez; Jason Siegel; Yi Ding; Matthew Castanier	5e. TASK NUMBER
	5f. WORK UNIT NUMBER
7. PERFORMING ORGANIZATION NAME(S) AND ADDRESS(ES)	8. PERFORMING ORGANIZATION REPORT NUMBER
Center For Automotive Research,3005 Boardwalk St,Ste 200 ,Ann Arbor,Mi,48108	**; #22630**
9. SPONSORING/MONITORING AGENCY NAME(S) AND ADDRESS(ES)	10. SPONSOR/MONITOR'S ACRONYM(S)
U.S. Army TARDEC, 6501 East Eleven Mile Rd, Warren, Mi, 48397-5000	**TARDEC**
	11. SPONSOR/MONITOR'S REPORT NUMBER(S) **#22630**

12. DISTRIBUTION/AVAILABILITY STATEMENT
Approved for public release; distribution unlimited

13. SUPPLEMENTARY NOTES
Submitted to IEEE Transactions on Control Systems Technology

14. ABSTRACT

Lithium ion batteries should always be prevented from overheating and hence thermal monitoring is indispensable. Since only the surface temperature of the battery can be measured, a thermal model is needed to estimate the core temperature of the battery, which can be higher and more critical. In this paper, an online parameter identification scheme is designed for a cylindrical lithium ion battery. An adaptive observer of the core temperature is then designed based on the online parameterization methodology and the surface temperature measurement. A battery thermal model with constant internal resistance is explored first. The identification algorithm and the adaptive observer is validated with experiments on a 2:3Ah 26650 lithium iron phosphate/graphite battery. The methodology is later extended to address temperature dependent internal resistance with non-uniform forgetting factors. The capability of the methodology to track the long term variation of the internal resistance is beneficial for battery health monitoring.

15. SUBJECT TERMS
Lithium ion battery, core temperature, adaptive estimation, state of health.

16. SECURITY CLASSIFICATION OF:			17. LIMITATION OF ABSTRACT	18. NUMBER OF PAGES	19a. NAME OF RESPONSIBLE PERSON
a. REPORT	b. ABSTRACT	c. THIS PAGE			
unclassified	**unclassified**	**unclassified**	**Public Release**	**11**	

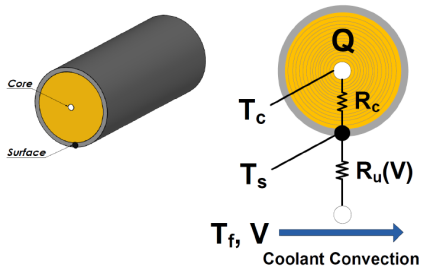

Fig. 1. Single Cell Radially Lumped Thermal Model

the SEI. Hence, the least square algorithm with non-uniform forgetting factors is also applied to track the long term growth of the internal resistance. The growth of the internal resistance can be viewed as an important indication of the state of health (SOH) of the battery, and used as a reference for the onboard battery management system to extend the life of the batteries. Parameterization of battery model and adaptive monitoring of the battery voltage and SOH have been explored previously in various seminal papers [15], [16], [17], but this paper is among the first ones to adaptively monitor the temperatures (especially the core temperature) of batteries and SOH from a thermal perspective.

II. Lumped Thermal Model of a Cylindrical Lithium Ion Battery

The radial thermal dynamics of a cylindrical battery are modeled based on the classic heat transfer problem by assuming heat generation located at the core and zero heat flux at the center, as shown in Fig. 1.

The two-state approximation of the radially distributed thermal model is defined as [9]

$$C_c\dot{T}_c = I^2R_e + \frac{T_s - T_c}{R_c} \tag{1a}$$

$$C_s\dot{T}_s = \frac{T_f - T_s}{R_u} - \frac{T_s - T_c}{R_c}, \tag{1b}$$

where the two states are the surface temperature T_s and the core temperature T_c. The temperature variation along the battery height is neglected here, assuming homogeneous conditions.

Heat generation is approximated as a concentrated source of Joule loss in the battery core, computed as the product of the current, I, squared and the internal resistance, R_e. The internal resistance R_e is considered as an unknown parameter to be identified. This simplification can lead to cycle-dependent values for lumped resistance R_e, or even non-constant resistance within a single cycle, because R_e can vary with conditions such as temperature, SOC and degradation [5], [10], [11], [13]. In subsequent sections, first, R_e will be identified online as a constant under a drive cycle, and then identification of R_e as a varying parameter will be addressed in Sec. (VII). Heat generation calculated based on an equivalent circuit model has also been used for thermal model parameterization in another ongoing work [18].

Heat exchange between the core and the surface is modeled by heat conduction over a thermal resistance, R_c, which is a lumped parameter aggregating the conduction and contact thermal resistance across the compact and inhomogeneous materials. A convection resistance R_u is modeled between the surface and the surrounding coolant to account for convective cooling. The value of R_u is a function of the coolant flow rate, and in some vehicle battery systems, the coolant flow rate is adjustable to control the battery temperature. Here, it is modeled as a constant as if the coolant flow rate is fixed to accommodate the maximum required cooling capacity. A model with the more complicated varying R_u has also been investigated in [19].

The rates of the temperature change of the surface and the core depend on their respective lumped heat capacity. The parameter C_c is the heat capacity of the jelly roll inside the cell, and C_s is related to the heat capacity of the battery casing.

The complete parameter set for this model includes C_c, C_s, R_e, R_c, and R_u, of which the values cannot be easily calculated. Consider the conduction resistance R_c as an example. Theoretically, R_c can be calculated based on the conductivity and dimensions of the wound cell electrode assembly and the aluminum casing. However, since the rolled electrodes are composed by the cathode, anode, current collectors and separator, it will be difficult to obtain an accurate value for the overall conductivity. Moreover, R_c also includes the contact thermal resistance between the rolled electrodes and the casing, which involves various contact properties adding to the complexity of the calculation.

Therefore, model identification techniques are developed in the following section to obtain the lumped phenomenological values of the model parameters based on measurable inputs and outputs of the model.

III. Parameterization Methodology

For model identification, a parametric model

$$z = \theta^T\phi \tag{2}$$

is derived first by applying Laplace transformation to the model, where z is the observation, θ is the parameter vector and ϕ is the regressor [20]. Both z and ϕ should be measured or can be generated from measured signals.

With a parametric model, various algorithms can be chosen for parameter identification, such as the gradient and the least squares methods. The method of least squares is preferred for noise reduction [20].

The recursive least squares algorithm is applied in an online fashion, as parameters are updated continuously [20]

$$\dot{\theta} = P\frac{\varepsilon\phi}{m^2}, \tag{3a}$$

$$\dot{P} = -P\frac{\phi\phi^T}{m^2}P, \tag{3b}$$

$$\varepsilon = z - \theta^T\phi, \tag{3c}$$

$$m^2 = 1 + \phi^T\phi, \tag{3d}$$

where m is a normalization factor that enhances the robustness of parameter identification.

In some cases, to make the observation z and the regressors ϕ proper (or causal), a filter $\frac{1}{\Lambda(s)}$ will have to be designed and applied. The parametric model will then become

$$\frac{z}{\Lambda} = \theta^T \frac{\phi}{\Lambda}. \tag{4}$$

The convergence and robustness of the identification are guaranteed if the regressors, ϕ in Eq. (8), are stationary signals and satisfy the persistent excitation (PE) conditions [20]. The PE conditions are satisfied if there exist some time interval T_0, and positive number α_1 and α_0, such that

$$\alpha_1 I_M \geq U(t) = \frac{1}{T_0}\int_t^{t+T_0} \phi(\tau)\phi^T(\tau)d\tau \geq \alpha_0 I_M \quad \forall t \geq 0, \tag{5}$$

where I_M is the identity matrix with the same dimension as U(t) [20]. This criteria can be used to test whether a drive cycle can ensure robust parameter convergence.

IV. Online Parameterization of the Battery Thermal Model

In this section, the parameterization scheme described previously is applied to the cylindrical battery thermal model in Eq. (1). A parametric model for identification can be derived by taking the Laplace transformation of Eq. (1) and replacing the unmeasured T_c with measured signals I, T_f, and T_s,

$$\begin{aligned} s^2T_s - sT_{s,0} \quad &= \tfrac{R_e}{C_cC_sR_c}I^2 + \tfrac{1}{C_cC_sR_cR_u}(T_f - T_s) + \tfrac{1}{C_sR_u}s(T_f - T_s) \\ &\quad - \tfrac{1}{C_cC_sR_c}\big((C_c+C_s)sT_s - C_sT_{s,0} - C_cT_{c,0}\big), \end{aligned} \tag{6}$$

where $T_{s,0}$ and $T_{c,0}$ are the initial surface and core temperatures. When the initial core temperature, $T_{c,0}$, is considered to be the same as the initial surface temperature, $T_{s,0}$, as if the battery starts from thermal equilibrium, Eq. (6) becomes

$$\begin{aligned} s^2T_s - sT_{s,0} &= \frac{R_e}{C_cC_sR_c}I^2 + \frac{1}{C_cC_sR_cR_u}(T_f - T_s) \\ &\quad - \frac{C_c+C_s}{C_cC_sR_c}(sT_s - T_{s,0}) + \frac{1}{C_sR_u}s(T_f - T_s). \end{aligned} \tag{7}$$

It is assumed here that T_f is regulated as a steady output of the air-conditioning unit and thus $sT_f = 0$, giving

$$\begin{aligned} s^2T_s - sT_{s,0} &= \frac{R_e}{C_cC_sR_c}I^2 + \frac{1}{C_cC_sR_cR_u}(T_f - T_s) \\ &\quad - \left(\frac{C_c+C_s}{C_cC_sR_c} + \frac{1}{C_sR_u}\right)(sT_s - T_{s,0}). \end{aligned} \tag{8}$$

If T_f is a time-varying input to the model, sT_f should not be dropped. In this case, T_f can also be used as an input excitation in the parametric model. A second order filter should be applied to the observation and the regressors in Eq. (8) to make them proper. The filter takes the form

$$\frac{1}{\Lambda(s)} = \frac{1}{(s+\lambda_1)(s+\lambda_2)}, \tag{9}$$

where λ_1 and λ_2 are the time constants of the filter. The values of λ_1 and λ_2 can be chosen to filter the noises with frequencies higher than the temperature dynamics.

For the parametric model in Eq. (8),

$$Z(s) = \frac{s^2T_s - sT_{s,0}}{\Lambda(s)} \tag{10a}$$

$$\Phi(s) = [\frac{I^2}{\Lambda(s)} \quad \frac{T_f - T_s}{\Lambda(s)} \quad \frac{sT_s - T_{s,0}}{\Lambda(s)}]^T \tag{10b}$$

$$\theta = [\alpha \quad \beta \quad \gamma]^T, \tag{10c}$$

where

$$\alpha = \frac{R_e}{C_cC_sR_c} \tag{11a}$$

$$\beta = \frac{1}{C_cC_sR_cR_u} \tag{11b}$$

$$\gamma = -\left(\frac{C_c+C_s}{C_cC_sR_c} + \frac{1}{C_sR_u}\right). \tag{11c}$$

For implementation in a practical system, the identification algorithm is formulated along with signals z and ϕ in the time domain based on Eq. (3), or in the discrete time domain based on equivalent formula. For example, $z(t)$, whose Laplace transform is $\frac{s^2T_s - sT_{s,0}}{\Lambda(s)}$, can be obtained by calculating the convolution of $T_s(t) - T_{s,0}$ and the inverse Laplace transform of $\frac{s^2}{\Lambda(s)}$. In this way, calculation of the 2nd order derivative of T_s, s^2T_s, which can be easily corrupted by noises, is avoided.

By using the parametric model in Eq. (8), only three lumped parameters, α, β and γ, can be identified under the condition of persistent input excitation[20]. Prior knowledge of two of the physical parameters must be assumed so as to determine a set of unique solution for the original five physical parameters, Cc, Cs, Re, Rc, and Ru from α, β and γ. Of the five physical parameters, the internal resistance R_e may vary due to aging and should be identified online. The conduction resistance R_c is difficult to estimate as explained previously. The convection resistance R_u will be influenced by the coolant flow conditions around the cell depending on the packaging. Therefore, it is not easy to obtain prior knowledge of those three parameters. The heat capacities C_c and C_s, which depend on the thermal properties and the mass of the rolled electrode assembly and the casing, are relatively constant over lifetime. In addition, the heat capacities will only affect the speed of transient response of the model without having any impact on the steady state temperatures. Consequently, the heat capacities C_c and C_s are selected to be the presumed parameters.

With C_c and C_s presumed and α, β and γ identified, R_e, R_c and R_u can be obtained by solving the following set of equations:

$$\beta(C_c+C_s)C_sR_u{}^2 + \gamma C_sR_u + 1 = 0 \tag{12a}$$

$$R_c = \frac{1}{\beta C_sC_cR_u} \tag{12b}$$

$$R_e = \alpha C_cC_sR_c. \tag{12c}$$

The quadratic equation for R_u in Eq. (12) can lead to two solutions, but the right one can be decided based on the coolant flow conditions based on [21].

The least squares algorithm in Eq. (3) can then be applied for parameter identification. In [19] and [22], the methodology

has been applied and verified by simulation with a battery thermal model with assumed parameters. In the following section, the parameterization is further validated by experiments.

V. Experiment Validation

A. Experiment Set-Up and Measurements

Experiments have been conducted to validate the designed parameterization scheme. A 2.3Ah $A123^{TM}$ 26650 $LiFePO_4$/graphite battery is cycled with a Bitrode^{TM} cycler under the control of a customized testing system by A&D Technology^{TM}. A Cincinnati Sub-Zero^{TM} environmental simulation chamber is used to regulate the temperature of the coolant air flow around the battery.

T-type thermocouples are installed both on the battery casing to measure its surface temperature, and also inside the battery core to measure the core temperature. During the fabrication process of the 26650 cylindrical cell, the electrode assembly is wound up to form a roll, leaving a cavity in the center. To measure the core temperature, the battery was drilled inside an argon-filled glove box through to its central cavity, where the thermocouple was inserted, as shown in Fig. 2. The battery was then sealed and taken out of the glove box for experiments.

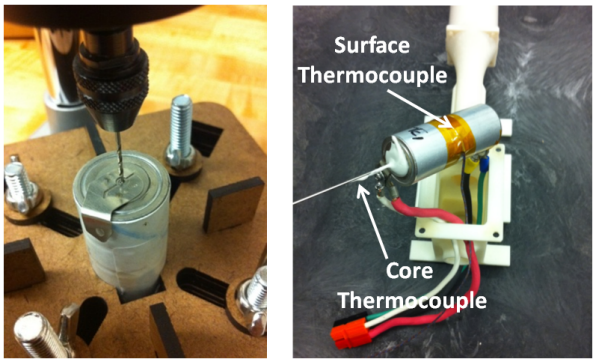

Fig. 2. Instrumentation of the Battery Core Temperature (left: drill press setup of the battery; right: installation of the thermocouples)

Inside the thermal chamber, the battery was placed in a designed flow chamber as shown in Fig. 3, where a fan was mounted at one end to regulate the air flow around the cell. The speed of the fan is controlled by Pulse Width Modulation (PWM) signals to change the air flow rate. The flow chamber is used to emulate the pack air cooling conditions where the coolant flow rate is adjustable (like in [19]). A T-type thermocouple is placed near the battery inside the flow chamber to measure the air flow temperature T_f.

B. Persistent Excitation of Input Signals

A driving cycle, the Urban Assault Cycle (UAC) [23], is applied as the current excitation to the battery in galvanostatic mode. The UAC is originally a velocity cycle for military vehicles. The current profile for a battery pack of a hybrid military vehicle under UAC is derived in [23] by applying a certain power management strategy. The type of battery used in the experiment ($LiFePO_4$ 26650) is different from the one in

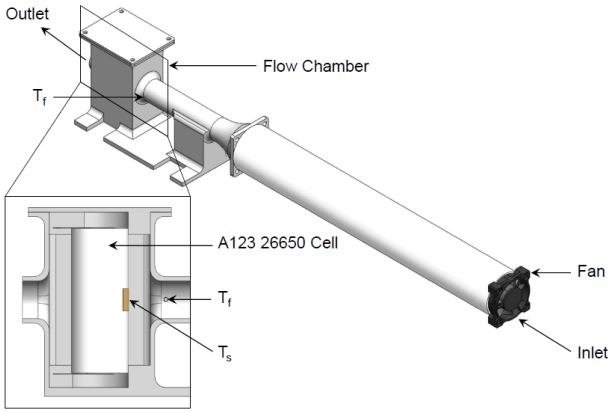

Fig. 3. Schematics of the Flow Chamber

[23], hence the UAC current cycle taken from [23] is rescaled for the experiments. The original 20-minute cycle is repeated 4 times to let the battery temperature reach periodic steady state. The resulting scaled drive cycle current is plotted in Fig. 4. The normalized unit of C-rate is commonly used to describe the load applied to the battery and 1 C corresponds to the magnitude of the current that depletes the battery in one hour (in this case 2.3 A). The negative current indicates the discharge of the battery as the energy is drawn from the battery to drive the vehicle, and the positive current represents the regenerative braking during which the battery is charged. The discharge load is fairly evenly distributed between 1 C and 7 C, except at around -8 C which indicates rapid acceleration. The charge load is mostly below 7C and occasionally reaches above 10 C during drastic braking. The SOC evolution under this cycle is also plotted in Fig. 4, showing a decrease from about 50% to roughly 35%.

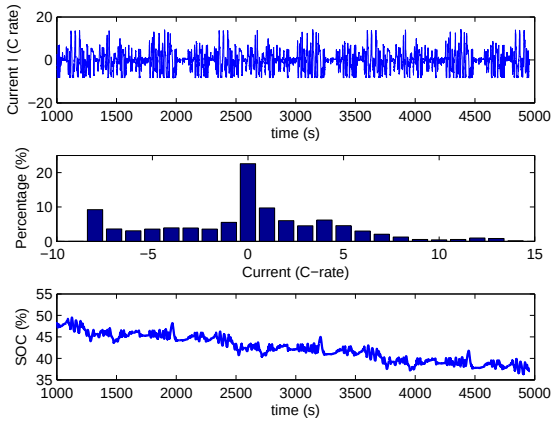

Fig. 4. Scaled UAC Current Excitation (top: currents in time series; middle: histogram of the currents; bottom: SOC variation under the cycle)

The temperature of the thermal chamber is controlled at 26 ^oC. The resulting battery surface temperature T_s and air flow temperature T_f are measured and recorded by the data acquisition system. The measured T_s and T_f under the scaled UAC cycles are plotted in Fig. 5, which along with I are then used for parameter identification.

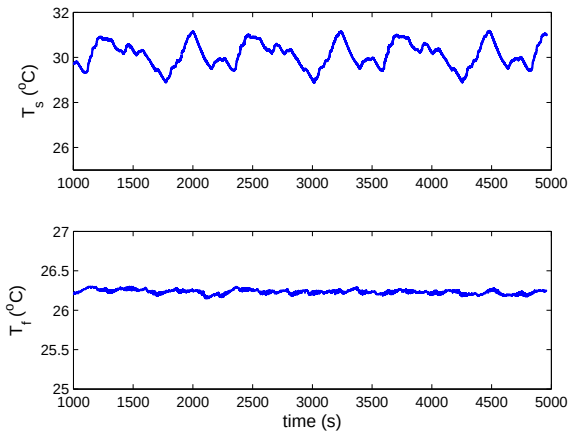

Fig. 5. Measured T_s and T_f under Scaled UAC Cycle (top: surface temperature T_s; bottom: flow temperature T_f)

The criteria in Eq. (5) is then applied to check if the UAC cycle satisfies the PE condition, which requires the regressors to be stationary signals first. As can be seen in Fig. 5, the surface temperature T_s will vary periodically after the battery finishes the warm-up phase at about 1000 second. Consequently, the regressors, which include I^2, $T_f - T_s$, and sT_s, will become stationary signals, as shown in Fig. 6. The U(t) matrix can then be calculated to check the persistent excitation conditions. It is noted that the measurements taken during the warm-up period can also be used for identification, even though they are not stationary signals [19].

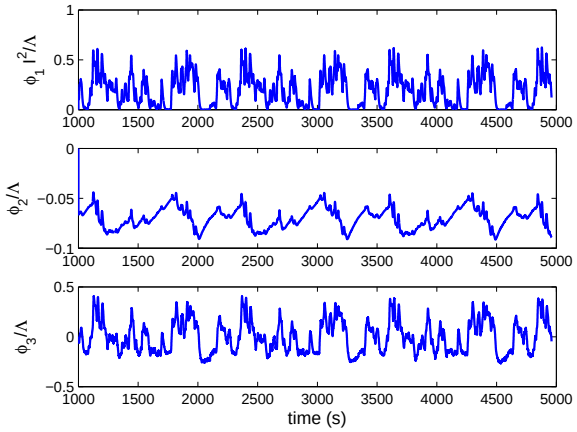

Fig. 6. Evolution of Regressors ϕ in Periodic Steady State

Since the current input consists of repeated UAC cycles (each lasting for 1200s), the values of U(t) only need to be calculated over a time interval $T_0 = 1200s$ for $1000s \leq t \leq 2200s$. It is noted that in this case, U(t) is not a diagonal matrix, and thus its eigenvalues are calculated to check the persistent excitation conditions. The smallest and the largest eigenvalues of U(t), λ_{max} and λ_{min}, are plotted in Fig. 7. It can be concluded from Fig. 7 that α_1 in Eq. (5) can be found as 0.086 s^{-1}, which is the maximum of $\lambda_{max}(t)$, and α_0 as 2.4×10^{-4} s^{-1}, which is the minimum of $\lambda_{min}(t)$. Consequently, under the UAC cycle,

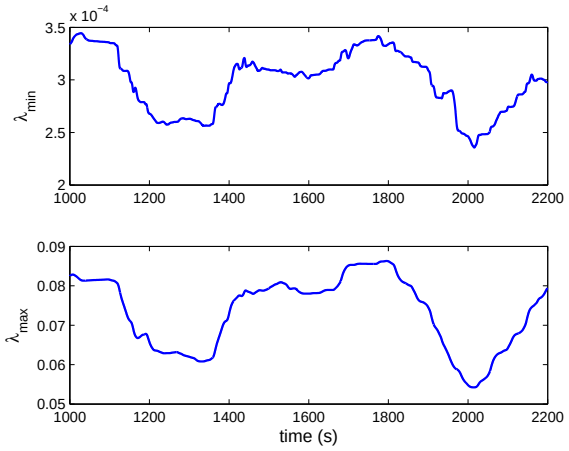

Fig. 7. Evolution of the Eigenvalues of U(t) in Steady State (Top: smallest eigenvalue; bottom: largest eigenvalue.)

TABLE I
INITIAL GUESS AND IDENTIFICATION RESULTS OF PARAMETERS

Parameters	$R_u(KW^{-1})$	$R_e(m\Omega)$	$R_c(KW^{-1})$
Initial Guess	1.5	30	0.5
ID Results	3.03	11.4	1.83

the regressors satisfy the conditions of persistent excitation. Furthermore, α_0 are related to the speed of the convergence for parameter identification. Specifically, when the gradient method is used, $2\alpha_0^{-1}$ is the upper limits of the time constant of the parameter convergence [20], which would be

$$\tau \leq 8333s \tag{13}$$

in this case. Based on Eq. (13), the 90% settling time for the convergence under the gradient search algorithm is expected to be less than 19186s. It is noted that 19186s is a rather conservative estimation of the convergence time, in real application, the convergence is usually accelerated by increasing the adaptive gain [20], [24].

C. Results and Discussion

The measured signals I, T_s and T_f in Fig. 4 and Fig. 5 are used for recursive least squares parameterization. The three parameters to be identified, R_u, R_e and R_c, are initialized with the initial guess values in Table I. For the heat capacity, the single C_p in [8] is split into C_c and C_s here representing the battery core and surface heat capacities respectively. The heat capacity of the battery core, C_c, is assumed to be 67 JK^{-1}, slightly smaller than C_p in [8]. The heat capacity of the battery surface, C_s, is assumed to be 4.5 JK^{-1} based on the dimensions of the aluminum casing of the 26650 battery and the specific heat capacity of aluminum.

The results of the recursive identification are plotted in Fig. 8. It is noted that the identification procedures are started after the first 1000 seconds when the temperature enters periodic steady state. It can be seen that starting at some random initial values, the 3 parameters converge to the values listed in

Table I. The upper plot in Fig. 8 shows the convergence of the lumped parameters α, β and γ in Eq. (8), and the lower plot shows the convergence of the physical parameters R_u, R_c and R_e, which are obtained by solving Eq. (12). It is noted that the convergence time is within the range (less than 19186 s) discussed in Sec. (V-B), which is strictly speaking only valid for the gradient method. The convergence rate is accelerated here by increasing the initial adaptive gain P_0 [24], [25], which is the initial value of $P(t)$ in Eq. (3).

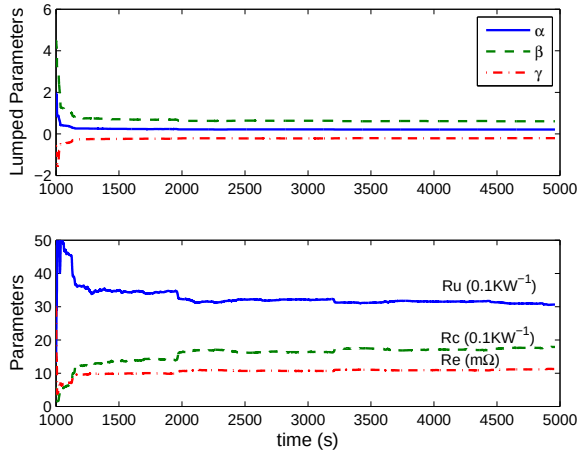

Fig. 8. On-line Parameter Identification Results (top: convergence of the lumped parameters; convergence of the original parameters)

For validation purpose, the identified parameters are applied to Eq. (1) to estimate both the battery surface temperature T_s and the core temperature T_c. The estimation is then compared with the measurement, as plotted in Fig. 9. The estimated surface temperatures T_s match the measurement exactly, since T_s is directly used for identification. It is noted that the measured core temperature T_c also agrees closely with the measured T_c (which was not used for parameterization), showing the capability of the parameterized model to predict the correct battery core temperatures. Once the parameterization scheme is validated, it can be run in onboard BMS to estimate the core temperatures in real time without actually measuring it (as in the lab set-up).

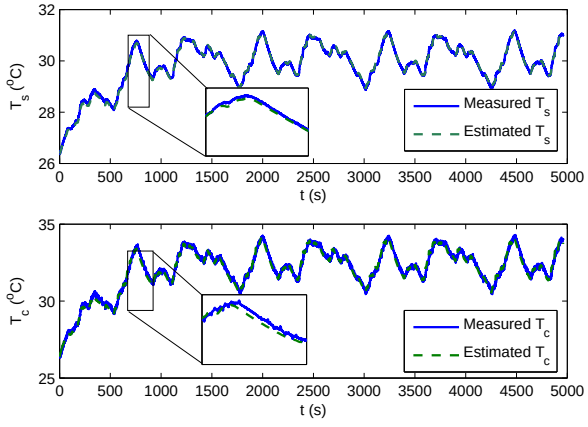

Fig. 9. Experimental Validation (top: estimated surface temperature T_s vs. measured; bottom: estimated core temperature T_c vs. measured)

TABLE II
COMPARISON OF THE IDENTIFIED PARAMTERS TO [8]

Parameters	Value	Equivalence in [8]	Value
$R_c(KW^{-1})$	1.83	$R_{in}(KW^{-1})$	$3.2 \sim 3.4$
$R_u(KW^{-1})$	3.03	$R_{out}(KW^{-1})$	$8.4 \sim 9.1$
$C_c(JK^{-1})$	67	$C_p(JK^{-1})$	$73 \sim 78$
$C_s(JK^{-1})$	4.5	-	-

The identification results are also compared to those in [8], where thermal parameters of the same battery are identified based on the measurement of both surface and the core temperatures under designed current inputs. In [8], the battery is modeled with a single dynamic state (the core temperature), and the surface temperature is related to the core temperature with an algebraic equation by assuming the surface heat capacity to be zero. In [8], the heat generation is pre-calculated by resistive heat dissipation (due to ohmic voltage drop) plus entropic heat, and in this work, the entropic heat is ignored and the heat generation is accounted for by multiplying the current square with an identified parameter R_e. It is noted that the entropic heat is generally small comparing to the resistive heat, especially in the middle SOC range here as shown in Fig. 4.

Table II summarizes the comparison between the thermal parameters identified in [8] and in this paper. It can be seen that the identified value of the conduction resistance (R_c) between the core and the surface is smaller than that in [8]. This is probably because the surface temperature in this work is measured at the aluminum casing instead of at the outside paper cover (as in [8]), which indicates better heat conduction. The identified convection resistance between the surface and the coolant R_u is significantly smaller than that in [8], which can be explained by the fact that during the experiment, the air flow is constantly blown into the flow chamber by the fan which enhances the convective cooling through the coolant air.

VI. Adaptive Battery Core Temperature Estimation

In control application, an observer is often designed based on a plant model to estimate the states of a plant, especially ones that are not measured, e.g. the core temperature T_c of the battery in this case. Such model based observers can be categorized as either an open loop observer or a closed loop observer. For a linear system

$$\dot{x} = Ax + Bu \tag{14}$$

where x are the states and u are the inputs, an open loop observer is simply

$$\dot{\hat{x}} = A\hat{x} + Bu, \tag{15}$$

as the estimated states $\hat{x}$ are calculated by the model solely based on the inputs u. For the battery thermal model specifi-

cally, we have

$$x = [T_c \quad T_s]^T \tag{16a}$$
$$u = [I^2 \quad T_f]^T \tag{16b}$$
$$A = \begin{bmatrix} -\frac{1}{R_c C_c} & \frac{1}{R_c C_c} \\ \frac{1}{R_c C_s} & -\frac{1}{C_s}(\frac{1}{R_c}+\frac{1}{R_u}) \end{bmatrix} \tag{16c}$$
$$B = \begin{bmatrix} \frac{R_e R_c}{C_c} & 0 \\ 0 & \frac{1}{R_u C_s} \end{bmatrix} \tag{16d}$$

However, the estimation by such open loop observer can often be corrupted by unknown initial conditions, and noises in the measurement of the inputs. To address such issues, a closed loop observer, such as a Luenberger observer or a Kalman filter, is often designed to estimate the states based on the model and the feedback of some measurable outputs [26],

$$\dot{\hat{x}} = A\hat{x} + Bu + L(y - \hat{y}) \tag{17a}$$
$$y = Cx + Du \tag{17b}$$
$$\hat{y} = C\hat{x} + Du \tag{17c}$$

where y are the measured system outputs, $\hat{x}$ and $\hat{y}$ are estimated states and output, L is the observer gain, and A, B, C and D are model parameters. For the battery thermal model, since the surface temperature T_s is measurable, we have

$$C = [0 \quad 1] \tag{18a}$$
$$D = \quad 0. \tag{18b}$$

It is noted that the difference between the measured and the estimated output is used as the feedback to correct the estimated states. Comparing with an open loop observer, the closed loop observer can accelerate the convergence of the estimated states to those of the real plant under unknown initial conditions, e.g. a Luenberger observer [26], or optimize the estimation by balancing the effect of unknown initial conditions and noises, e.g. a Kalman filter [27].

By taking the structure of a closed loop observer, an adaptive observer is then designed based on certainty equivalence principle [20],

$$C_c \dot{\hat{T}}_c = \quad I^2 \hat{R}_e + \frac{\hat{T}_s - \hat{T}_c}{\hat{R}_c} + l_1(T_s - \hat{T}_s) \tag{19a}$$
$$C_s \dot{\hat{T}}_s = \frac{T_f - \hat{T}_s}{\hat{R}_u} - \frac{\hat{T}_s - \hat{T}_c}{\hat{R}_c} + l_2(T_s - \hat{T}_s), \tag{19b}$$

where $\hat{T}_s$ and $\hat{T}_c$ are the estimated surface and core temperatures, and the observer parameters $\hat{R}_e$, $\hat{R}_c$ and $\hat{R}_u$ are taken from the online identification results in Sec. (V). The block diagram of the adaptive observer is shown in Fig. 10. The input current I, coolant temperature T_f, and the measured surface cell temperature T_s are fed into the parameter identifier to estimate model parameters R_u, R_e and R_c. The adaptive observer uses the estimated parameters to estimate the core and the surface temperatures. The estimated T_s is compared to the measurement and the error is fed back to correct the core temperature and surface temperature estimation. The estimations for both parameters and temperatures are updated at each time step.

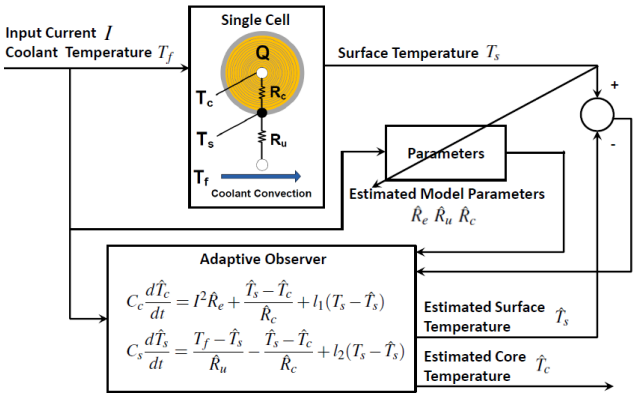

Fig. 10. On-line Identification Scheme and Adaptive Observer Structure

The data in Sec. (V) are used to test the response of the adaptive observer, as plotted in Fig. 11. The initial estimated temperatures of the adaptive observer are set at 30 ^oC for both the surface and the core, whereas the correct value is 26 ^oC, and the parameters are initialized with the initial guess values in Table I. It can be seen from Fig. 11 that the estimated surface temperature T_s converges to the actual values much faster than the core temperature T_c. The reason is that the surface temperature T_s is accessible by the adaptive observer both via parameter identification and closed loop error feedback, and thus the observer can adjust its estimation of T_s quickly based on direct reference of the measurement. But for the core temperature T_c, which is not measured, its estimation accuracy depends on the accuracy of the model parameters. Therefore, the convergence of T_c to the actual values will only happen after the identified parameters converge to the correct model parameters (at approximately 3000 seconds).

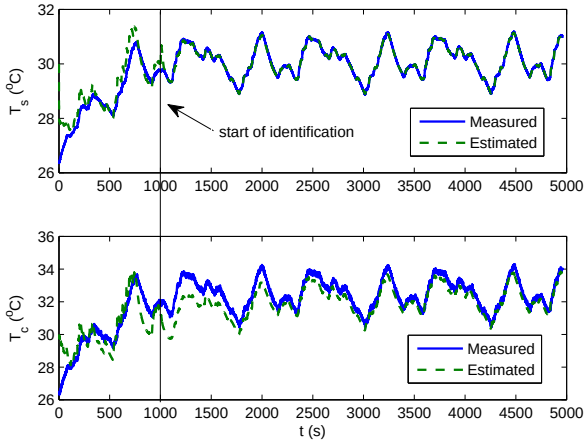

Fig. 11. Response of the Closed loop Adaptive Observer (top: adaptive estimation of the surface temperature vs. measurement; bottom: adaptive estimation of the core temperature vs. measurement)

VII. Parameterization of the Battery Thermal Model with Temperature Dependent R_e

For most lithium ion batteries, their internal resistance R_e depends on temperature and SOC, [5], [6], [11]. In general

cases, R_e is high when the temperatures are low and when the SOC is close to 0% or 100%. An Arrhenius function is often used to describe the relationship between R_e and the battery (core) temperature T_c, as

$$R_e = R_{e,ref} \exp\left(\frac{T_{ref}}{T_c}\right), \tag{20}$$

where $R_{e,ref}$ is the reference resistance value at a certain reference temperature T_{ref}, and T_{ref} and T_c are in K. It is noted that the change in resistance with respect to SOC is negligible in the normal vehicle battery operating range ($20\% - 80\%$ SOC) and thus is not considered here. The relationship between R_e and T_s described by Eq. (20) is plotted in Fig. 12, by taking $R_{e,ref} = 0.091\ m\Omega$ and $T_{ref} = 1543\ K$.

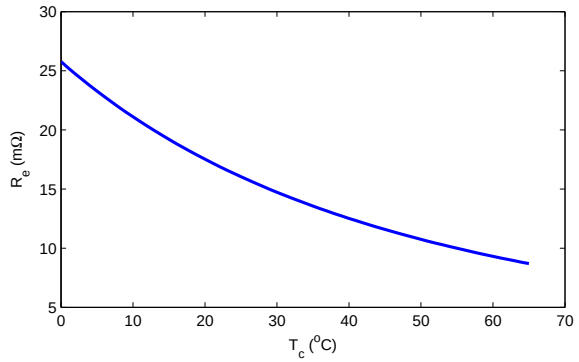

Fig. 12. Dependence of R_e on T_c

As a result, in real application, R_e will be varying as the temperature fluctuates. Such variation can not be neglected when the power demands are high and dramatically varying. Simulation is used in this section for illustration. Simulated variation of R_e due to T_c fluctuation under a drastic current cycle is shown in Fig. 13. It can be seen that the drastic current

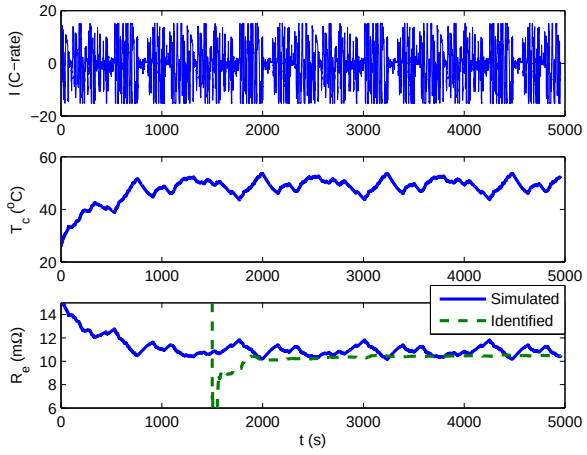

Fig. 13. Errors in R_e Estimation when the Temperature Varies Significantly (top: drive cycle current; middle: fluctuation of the battery core temperature; bottom: errors in R_e identification)

variation creates a 10 ^oC of fluctuation in the battery core temperature T_c. The resulting variation of R_e is about 20% as shown by the blue line in the bottom plot of Fig. 13.

Since the least squares identification algorithm in Eq. (3) identifies each parameter as a constant, when R_e is varying, errors will be observed in R_e identification as shown in Fig. 13. This will not only introduce errors in R_e estimation but might also affect the estimation of other parameters, and eventually corrupt the estimation of the core temperature T_c. To address such issue, a least squares algorithm with forgetting factors is then designed to identify R_e as a time-varying parameter.

A. Identification Design with Forgetting Factor

When forgetting factors are adopted, most parts of the least square algorithm will be the same as Eq. (3), except that

$$\dot{P}(t) = \eta^T P(t)\eta - P(t)\frac{\phi(t)\phi^T(t)}{m^2(t)}P(t), \tag{21}$$

where η is the forgetting factor matrix [20].

The least square identification algorithm tries to find the optimal parameters that best fit the inputs and outputs over the whole data set. A pure least square algorithm treats each data point as equal, no matter if it is acquired most recently, or obtained much earlier. However, when a forgetting factor is applied, the data points will be weighted differently. Specifically, the newly acquired data are favored over the older ones. In the form shown in Eq. (21), the weight of the data will decay exponentially with the time elapsed, and the larger the forgetting factor is, the faster the decay will be. Consequently, the least square algorithm can track the parameters when they are time-varying.

The least square algorithm with forgetting factors can be applied to the original linear parametric model in Eq. (7). Of the three lumped parameters, namely α, β, and γ in Eq. (7), only α is related to time varying R_e, and all the others are constant. Therefore, non-uniform forgetting factors should be adopted with the η matrix designed as

$$\eta = \begin{bmatrix} \eta_1 & 0 & 0 \\ 0 & 0 & 0 \\ 0 & 0 & 0 \end{bmatrix}, \tag{22}$$

where η_1 is the forgetting factor associated with α (and hence R_e).

Simulation is conducted with $\eta_1 = 0.25$, and the results of identification are shown in Fig. 14. It can be seen that that the identified R_e can follow the simulated varying R_e after the recursive least squares online identification with forgetting factors is activated at 1500s. As shown in Fig. 15, the adaptive observer, taking the structure in Eq. (19) and parameters identified online (now R_e varying as shown in the bottom plot of Fig. 14), can estimate the battery core temperature T_c accurately after the identified R_e converges to the simulated R_e at around 3700s.

VIII. Degradation Detection by Monitoring Growth in Internal Resistance

The recursive least square algorithm with forgetting factors can also track the long term growth of the internal resistance, which can be used as an indication for the state of health (SOH) of the battery.

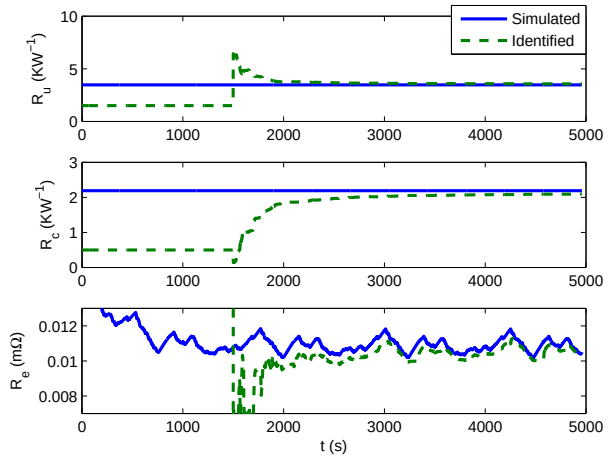

Fig. 14. Identification of Temperature Dependent Internal Resistance by the Least Square Algorithm with Non-uniform Forgetting Factors

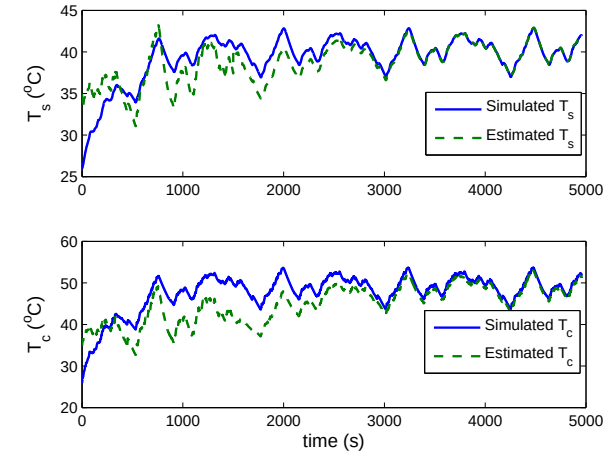

Fig. 15. Adaptive Estimation of Battery with Temperature Dependent Internal Resistance by Forgetting Factors (top: estimation of surface temperature T_s; bottom: estimation of core temperature T_c)

The growth of the internal resistance due to degradation is a process that occurs slowly over the battery lifetime. The internal resistance might increase substantially over hundreds of cycles or days according to [12], [13] and [14].

In this paper, the growth in internal resistance due to degradation is simulated and used to test the capability of the identification algorithm to detect the slow increase of the resistance. The internal resistance R_e, originally a function of the core temperature T_c, is now augmented with a term which is linearly increasing over time. The drive cycle used for simulation is the same as shown in the upper plot of Fig. 13, but is repeated for 350 times and the rate of growth in internal resistance is set at 0.14%/cycle. Although not modeled here, the rate of degradation may also increase with the temperature according to [12], [13] and [14].

The results of the online identification are shown in Fig. 16. It can been seen from Fig. 16 that the simulated internal resistance gradually increases over time while still subject to short-term variation due to the fluctuation of the battery core temperature. The identified R_e follows both the long-term and short-term variation of the simulated one with a small delay as shown in the inset of Fig. 16. In real vehicle application, since R_e is varying all the time, it is difficult to evaluate SOH by the instantaneous value of R_e and the averaged R_e might be a better choice instead. The mean value of R_e for each UAC cycle is plotted in the lower half of Fig. 16. It is noted that the averaged R_e can capture the long-term increase of the internal resistance and the identified value is a good estimation of the real one.

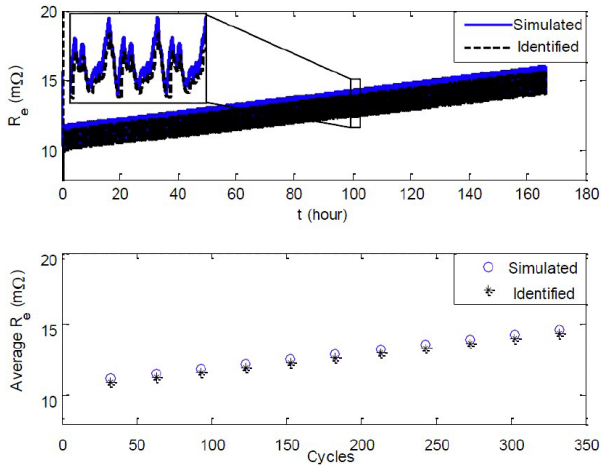

Fig. 16. (Simulated) Identification of Internal Resistance Subject to Degradation (top: identification of R_e with both short-term and long-term variation; bottom: simulated and identified cycle-average R_e)

The adaptive monitoring of the temperatures is also shown in Fig. 17. It is noted that as the internal resistance of the battery grows, the temperatures will also be elevated due to the increase of the heat generated. Since the observer is updated with the identified R_e in real time, it estimates both the core and the surface temperatures with high accuracy.

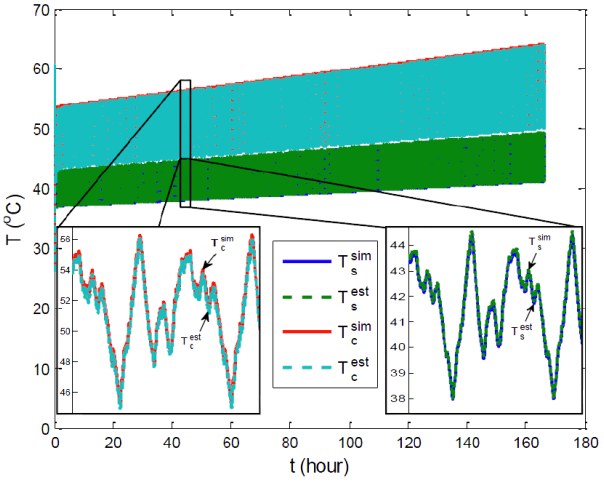

Fig. 17. Adaptive Estimation of Battery Subject to Degradation

IX. Conclusion

The core temperature of a lithium ion battery, which is usually not measurable, is of great importance to the onboard

battery management system, especially when the batteries are subject to drive cycles with high C-rate. The core temperature can be estimated by a two states thermal model, and the parameters of the models are critical for the accuracy of the estimation. In this paper, an online parameter identification scheme based on least square algorithm is designed for a cylindrical lithium ion battery thermal model. The online identification scheme can automatically identify model parameters based on the commonly available onboard signals. The updated parameters are then used to predict the unmeasured core temperature using a model based observer as shown with an A123 26650 lithium iron phosphate battery.

When the internal resistance of the battery is temperature dependent, which is a more realistic situation, the least square algorithm is augmented with non-uniform forgetting factors. The algorithm with forgetting factors can not only track the time-varying internal resistance, but also guarantee unbiased identification of the remaining constant parameters. The online parameterization also shows the capability to track the long-term variation of the internal resistance due to aging or degradation/abuse. The growth in internal resistance can be used for the SOH monitoring of the batteries. The methodology developed has been verified with simulations and is to be validated with experiments in the immediate future.

Applications, such as HEV, BEV and PHEV, usually have hundreds, or even thousands, of battery cells in series to meet their high power and energy requirements. Hence the vehicle level battery thermal management will be performed on a module basis, instead of on a cell basis. The single cell thermal model used in this paper can be scaled up to a pack model by considering cell to cell thermal interaction, and the parameterization methodology and the adaptive observer design will be investigated for the pack level model. Initial results of this work can be found in [22].

ACKNOWLEDGMENT

This work has been partially supported by the Ford Motor Company (Ford/UMICH Alliance Project) and the Automotive Research Center (ARC), a U.S. Army center of excellence for modeling and simulation of ground vehicles.

UNCLASSIFIED: Dist A. Approved for public release.

REFERENCES

[1] C. Y. Wang and V. Srinivasan, "Computational battery dynamics (cbd) – electrochemical/thermal coupled modeling and multi-scale modeling," *Journal of Power Sources*, vol. 110, pp. 364–376, 2002.

[2] S. A. Hallaj, H. Maleki, J. Hong, and J. Selman, "Thermal modeling and design considerations of lithium-ion batteries," *Journal of Power Sources*, vol. 83, pp. 1–8, 1999.

[3] H. Maleki and A. K. Shamsuri, "Thermal analysis and modeling of a notebook computer battery," *Journal of Power Sources*, vol. 115, pp. 131–136, 2003.

[4] W. B. Gu and C. Y. Wang, "Thermal-electrochemical modeling of battery systems," *Journal of The Electrochemical Society*, vol. 147, pp. 2910–2922, 2000.

[5] R. Mahamud and ChanwooPark, "Reciprocating airflow for li-ion battery thermal management to improve temperature uniformity," *Journal of Power Sources*, vol. 196, pp. 5685–5696, 2011.

[6] K. Smith and C.-Y. Wang, "Power and thermal characterization of a lithium-ion battery pack for hybrid-electric vehicles," *Journal of Power Sources*, vol. 160, p. 662C673, 2006.

[7] D. Bernardi, E. Pawlikowski, and J. Newman, "A general energy balance for battery systems," *J. Electrochem. Soc.*, vol. 132, pp. 5–12, 1985.

[8] C. Forgez, D. V. Do, G. Friedrich, M. Morcrette, and C. Delacourt, "Thermal modeling of a cylindrical lifepo4/graphite lithium-ion battery," *Journal of Power Sources*, vol. 195, pp. 2961–2968, 2010.

[9] C. W. Park and A. K. Jaura, "Dynamic thermal model of li-ion battery for predictive behavior in hybrid and fuel cell vehicles," in *SAE 2003-01-2286*, 2003.

[10] K. Smith, G.-H. Kim, E. Darcy, and A. Pesaran, "Thermal/electrical modeling for abuse-tolerant design of lithium ion modules," *International Journal of Energy Research*, vol. 34, p. 204C215, 2009.

[11] Y. Hu, S. Yurkovich, Y. Guezennec, and B. Yurkovich, "Electro-thermal battery model identification for automotive applications," *Journal of Power Sources*, vol. 196, pp. 448–457, 2011.

[12] T. Yoshida, M. Takahashi, S. Morikawa, C. Ihara, H. Katsukawa, T. Shiratsuchi, and J. ichi Yamakic, "Degradation mechanism and life prediction of lithium-ion batteries," *Journal of The Electrochemical Society*, vol. 153, pp. A576–A582, 2006.

[13] Z. Li, L. Lu, M. Ouyang, and Y. Xiao, "Modeling the capacity degradation of lifepo4/graphite batteries based on stress coupling analysis," *Journal of Power Sources*, vol. 196, pp. 9757–9766, 2011.

[14] J. Hall, A. Schoen, A. Powers, P. Liu, and K. Kirby, "Resistance growth in lithium ion satellite cells. i. non destructive data analyses," in *208th ECS Meeting MA2005-02, October 16-October 21, 2005 , Los Angeles, California*, 2005.

[15] A. P. Schmidt, M. Bitzer, and L. Guzzella, "Experiment-driven electrochemical modeling and systematic parameterization for a lithium-ion battery cell," *Journal of Power Sources*, vol. 195, pp. 5071–5080, 2010.

[16] M. Verbrugge and E. Tate, "Adaptive state of charge algorithm for nickel metal hydride batteries including hysteresis phenomena," *Journal of Power Sources*, vol. 126, pp. 236–249, 2004.

[17] B. Saha, K. Goebel, S. Poll, and J. Christophersen, "Prognostics methods for battery health monitoring using a bayesian framework," *IEEE Transactions on Instrumentation and Measurement*, vol. 58, pp. 291–296, 2009.

[18] H. E. Perez, J. B. Siegel, X. Lin, A. G. Stefanopoulou, Y. Ding, and M. P. Castanier, "Parameterization and validation of an integrated electro-thermal lfp battery model," in *ASME Dynamic Systems and Control Conference (DSCC)*, 2012.

[19] X. Lin, H. E. Perez, J. B. Siegel, A. G. Stefanopoulou, Y. Li, and R. D. Anderson, "Quadruple adaptive observer of li-ion core temperature in cylindrical cells and their health monitoring," in *American Control Conference*, 2012.

[20] P. A. Ioannou and J. Sun, *Robust Adaptive Control*. Prentice Hall, 1996.

[21] A. Zukauskas, "Heat transfer from tubes in crossflow," *Advances in Heat Transfer*, vol. 8, pp. 93–160, 1972.

[22] X. Lin, H. E. Perez, J. B. Siegel, A. G. Stefanopoulou, Y. Ding, and M. P. Castanier, "Parameterization and observability analysis of scalable battery clusters for onboard thermal management," *(Journal of) Oil & Gas Science and Technology-Revue d'IFP Energies nouvelles, France (Accepted)*, 2012.

[23] T.-K. Lee, Y. Kim, A. G. Stefanopoulou, and Z. Filipi, "Hybrid electric vehicle supervisory control design reflecting estimated lithium-ion battery electrochemical dynamics," in *American Control Conference*, 2011.

[24] J. Windsor, L. Silverberg, and G. Lee, "Convergence rate analysis of a multivariable recursive least squares parameter estimator," in *American Control Conference*, 1994.

[25] A. Astrom and B. Wittenmark, *Adaptive Control*. Addison Wesley, 1989.

[26] R. Williams and D. Lawrence, *Linear state-space control systems*. Wiley, 2007.

[27] R. E. Kalman, "A new approach to linear filtering and prediction problems," *Transactions of the ASME Journal of Basic Engineering*, vol. 82 (Series D), pp. 35–45, 1960.

Xinfan Lin received his B.S. and M.S. degree in Automotive Engineering from Tsinghua University, Beijing, China, in 2007 and 2009. He is currently a Ph.D. candidate in the Department of Mechanical Engineering at the University of Michigan, Ann Arbor. His research interests are in thermal modeling, identification and estimation of lithium ion batteries, and detection of imbalance in battery strings.

Hector E. Perez received the B.S. degree in Mechanical Engineering from California State University, Northridge in 2010. He is currently working on his M.S.E. degree as a Graduate Student Research Assistant in Mechanical Engineering at the University of Michigan. He is a recipient of the GEM Fellowship, sponsored by the Oak Ridge National Laboratory and the University of Michigan. His research interests lie in the experimental validation of electro-thermal lithium ion battery models.

Jason B. Siegel received his B.S., M.S., and Ph.D. degrees from the University of Michigan in 2004, 2006 and 2010 respectively. He is currently a Postdoctoral Research Fellow at the University of Michigan in the Powertrain Control Laboratory. His research interests are in modeling and control of alternative energy storage and conversion systems for automotive applications.

Anna G. Stefanopoulou is a professor of Mechanical Engineering and the Director of the Automotive Research Center at the University of Michigan. She was an assistant professor (1998-2000) at the University of California, Santa Barbara and a technical specialist (1996-1997) at Ford Motor Company. She is an ASME and an IEEE Fellow. She has a book, nine US patents, 4 best paper awards and more than 200 publications on estimation and control of internal combustion engines and electrochemical processes such as fuel cells and batteries.

Yonghua Li received his Ph.D. on control theory and applications from Beijing University of Aeronautics and Astronautics. He has since held numerous positions in academia and industry, most recently as a research engineer with the Research and Advanced Engineering Division of Ford Motor Company in Dearborn, Michigan, USA. His research interests include supervisory control of discrete event systems, automotive engine control, hybrid vehicle control, and automotive traction battery management system. He has published a number of papers and has been awarded several US patents.

R. Dyche Anderson is a Technical Expert for Battery Controls at Ford Motor Company leads the Advanced Battery Controls & Systems group in Ford Research & Advanced Engineering. Mr. Anderson has 25 years of experience in batteries, battery controls, and battery systems at both Ford and the Naval Surface Warfare Center/Crane. Mr. Anderson has worked in a wide variety of battery chemistries, including primary, secondary, and reserve systems. He has spent much of his career in product development, having product responsibility in batteries, battery systems, and battery controls, and has delivered batteries, battery controls, and/or battery systems for automotive, missile, and other applications. Mr. Anderson has a B.S. ChE. degree from Michigan Technological University and an M.S. (Chemical Engineering) degree from New Mexico State University, holds two patents in battery controls technology, has been author or co-author of numerous papers, and developed the internal battery controls training course used globally at Ford.

Yi Ding is an electrical engineer at the Ground Vehicle Power & Mobility, Tank Automotive Research and Engineering Center. His role is to monitor the energy storage research and development status and assist the energy storage team in monitoring the technical progress of R&D projects. He has more than 20 years of experience in battery research & development and project management.

Matthew P. Castanier is a Research Mechanical Engineer at the U.S. Army Tank Automotive Research, Development, and Engineering Center (TARDEC). His current research interests include reduced-order modeling of ground vehicle structures, modeling and simulation of automotive energy storage systems, and multidisciplinary design optimization. Dr. Castanier joined TARDEC in September 2008. Prior to that, he was a research faculty member for 12 years in the Department of Mechanical Engineering at the University of Michigan. Dr. Castanier received his B.S., M.S., and Ph.D. degrees in 1989, 1992, and 1995, all from the University of Michigan. He has published more than 30 articles in archival journals and over 75 papers in refereed conference proceedings.